IEEE Access
Multidisciplinary ⋮ Rapid Review ⋮ Open Access Journal

Received August 19, 2019, accepted September 4, 2019, date of publication September 6, 2019,
date of current version September 25, 2019.

Digital Object Identifier 10.1109/ACCESS.2019.2939977

Shape Decision-Making in Map-Like Visualization Design Using the Simulated Annealing Algorithm

TINGHUA AI[1], RUI XIN[1], XIONGFENG YAN[2], MIN YANG[1], AND BO AI[3]
[1]School of Resources and Environmental Science, Wuhan University, Wuhan 430072, China
[2]College of Surveying and Geo-Informatics, Tongji University, Shanghai 200092, China
[3]College of Geomatics, Shandong University of Science and Technology, Qingdao 266590, China

Corresponding author: Rui Xin (xinrui@whu.edu.cn)

This work was supported in part by the National Key Research and Development Program of China under Grant 2017YFB0503500, and in part by the National Natural Science Foundation of China under Grant 41531180.

ABSTRACT Semantic information without spatial characteristics can also be visualised in the form of a map. This map type is usually called map-like visualisation; it is not a representation of a real geo-entity but borrows the map metaphor. In current map-like visualisation works, the manipulation of the cartographic process is poor, and there is a considerable amount of randomness and uncertainty in the map results. For instance, in the process of converting semantic objects to map objects, the map shape is usually uncertain and has many possibilities. Frequently, however, we need shapes to follow certain principles, such as the principles of being close to a certain shape and having a simple geometry, to facilitate recognition and mapping. To achieve a balance between uncertain shapes and design needs, this study enhances the realisation of the cartographer's design idea by improving the controllability in the cartographic process. An optimisation technology, the simulated annealing algorithm, is introduced to control the determination of shape to improve mapping efficiency. Experiments based on real data show that based on this method, the map-like representation not only creates a whole outline close to the pre-defined shape but also realises internal regions with a simple shape.

INDEX TERMS Map-like visualisation, spatialization, uncertain shape, simulated annealing algorithm, map design.

I. INTRODUCTION

Regarding space, we usually refer to the space of the concrete physical world. However, from the broad perspective of all the kinds of spaces that we deal with, in addition to physical space, there are virtual information spaces composed of digital, textual and other semantic data that have abstract and multi-dimensional characteristics. Regardless of the type of space, the visualisation of space is important for understanding the space. Mapping provides representations for converting entities and phenomena from an original space to a conceptual world. If the original objects to be mapped belong to physical space, we obtain a common map that depicts their spatial location and other spatial characteristics. However, the objects to be mapped can be abstract semantic information in virtual information spaces, for instance, pure text information consisting solely of words and numbers without location information. They can also be represented in a map-like form by entities consisting of map symbols. This approach is usually called map-like visualisation; it borrows the cartographic method to create representations of non-spatial phenomena.

Using a map as a data expression vector enables people to observe abstract data by map browsing. Additionally, spatial symbols can be used to represent abstract semantic features through the map metaphor [40]. Map-like visualisation reduces or even avoids the pre-training process for the audience. Some studies have shown that even pre-school children have well-developed essential map-reading abilities [9]. In addition, centuries of accumulated cartographic knowledge combined with modern cartographic technology will provide powerful support for the expression and analysis of non-spatial data [5], [42]. Applying a map to non-spatial data not only provides new perspectives and new ideas for

The associate editor coordinating the review of this manuscript and approving it for publication was Laxmisha Rai.

solving problems but also increases the application scenarios of the map and widens the scope of its application.

Correspondingly, there is a special concept for describing this map-like representation process of non-spatial data: spatialization [44]. Usually, what we call spatialization is a very broad concept. According to the research object, it can be divided into spatialization of geographically referenced data and spatialization of non-geographically referenced data [44]. The data in the former are related to geographical location. For instance, the spatialization of demographic statistics [50], the spatialization of CO_2 distribution [25], spatialization of indicator values in spatial computing [54] etc. There are also some studies that research spatialization of video data [31] belongs to this data type, for instance, retrieval and analysis using geo-tags of videos [24]. However, this study focuses on the spatialization of non-geographically referenced data that have no geographic coordinates, and the data are also not related to geographical location. In particular, the subsequent spatialization in this article refers to the spatialization of non-geographically referenced data.

Spatialization transforms data from high-dimensional abstract space to low-dimensional visual space for data that do not contain spatial attributes, and it uses human potential experience to promote data representation and mining in the form of spatial objects [43]. From birth, spatial concepts are important ideas for understanding the world through our instinctive abilities of spatial cognition [16], [37]. The establishment of spatial height, low, size, distance, volume and others by visual cognition is able to depict other concepts by metaphor transform. Because people have a rich feeling and understanding of visible and spatial objects, when they convert abstract data into the form of spatial objects, human spatial thinking can play an important role. At the very beginning, spatial metaphors are often used as a rhetorical device in natural language; they use a spatial entity or spatial relation to represent certain abstract concepts [27]. In natural language, we usually use mountains, rivers, roads and other spatial entities to depict certain abstract phenomena via the method of metaphor; for example, ''Fame, like a river, is narrowest at its source and broadest farther off''. Maps, which are often called the second language in geo-science studies, can also be used to visualise abstract information through spatialization. Thus, we can understand an abstract concept and further reason or make decisions through intuitive physical spatial relations or associations [10].

Regarding theoretical research on spatialization, some studies have investigated issues related to uncovering the cognitive underpinnings of spatialization and have made important progress [17]–[19], [32]. Fabrikant and Skupin [20] proposed a spatialization framework based on geovisualisation and illustrated the framework with examples of spatialization. Such studies provide a great cognitive theoretical basis for subsequent spatialization practice. A great deal of practical research has been carried out in this field. Skupin [40] and Skupin *et al.* [45] used self-organising mapping (SOM) to classify text data items in a two-dimensional plane, divided spatial regions by clustering boundaries, and expressed these high-dimensional data in the form of maps. However, it is difficult to adjust the positions of data items and the shapes of map regions cannot be controlled by SOM method. In the above methods, the processing object is generally unstructured data. Structured data, such as data with a hierarchical structure and an association structure, are also the key research object of spatialization. For hierarchical data such as Wikipedia data, Biuk-Aghai and Ao [6] generated maps using the polygon expansion algorithm based on liquid modelling and proposed an enhancement method in a follow-up study [8]. In addition, Biuk-Aghai *et al.* [7] and [53] used a random filling method to build a map in a hexagon base map. It is difficult for the above methods to effectively control the expansion boundary of maps. Sometimes there are large gaps between map regions. Auber *et al.* [4] and Wattenberg [49] used space filling curves to guide regional division to construct map-like visualisations that can avoid large gaps among map regions and realise seamless regional splicing. At the same time, this kind of method has a certain controllability. For associated data, researchers have conducted a series of explorations with regard to converting graphs into maps [21], [23]. For social media data, which are typically associated data, researchers have used map-like visualisation to explore the information diffusion pattern and the evolution of major events in the network [13], [14]. Other studies have also used maps as a data expression vector to explore abstract data [15], [30], [38]. All of these studies provide good technical support for the spatialization display of non-spatial abstract data.

In current practical studies of map-like visualisation, more attention is paid to visualisation and generation techniques, but less attention is paid to map design. Maps are the combination of engineering and art. Map building and generation technology is of course essential. However, as a map-related study, certain efforts need be devoted to map-related design to promote the transmission and recognition of information. In addition, the poor controllability of the cartographic process leads to map results in which the randomness is too great. In the above studies, there is little artificial control over the mapping process. The mapping process mostly inputs data into the appropriate tools and then waits for the output of the results. The intermediate process is similar to a black box. In these current studies, mapping methods or tools provide only the layout rules of abstract data, and the data cannot be further manipulated in the mapping process. It is difficult for the cartographer to adjust and optimise the map results based on his or her own ideas. This lack of controllability in the mapping process will also be detrimental to the implementation of map design.

This study makes full use of the randomness in map-like visualisation and focuses on improving the controllability of map-like visualisation design. It presents a method for designing geometric shapes in map generation. On the one hand, a map outline is designed with the help of a similarity measure algorithm to improve the map recognition of

map-like works. On the other hand, the shape of the internal region is adjusted to facilitate the transmission and cognition of information. This shape design process is optimised by using a simulated annealing algorithm to improve efficiency. The rest of this paper is organised as follows. In Section II, we first discuss the basic ideas of our study. Section III illustrates the specific design approaches to map outlines and regions. We perform relevant experiments to verify our method in Section IV. Finally, the conclusions of this study and possible avenues of future research are provided in Section V.

II. BASIC IDEAS

The purpose of map-like visualisation is to convey information through another representation by map carriers, similar to visual metaphors [36]. In map design, human cognition plays an important role. Some cognition models have been established for human cognitive behaviour, such as the model human processor (MHP) by Card *et al.* [12] and the novice's information visualisation sensemaking (NOIVS) model by Lee *et al.* [28]. Through experiments, researchers find that a map metaphor is processed by humans in the early stages of the cognitive process [34]. During this stage, the audience first constructs an overall visual frame of the image and then combines memory, personal experience and knowledge in the mind to carry out the visual exploration process. This cognitive process is similar to the theory of gestalt cognition, in which people's perception of things extends from the whole to the details. Thus, the first impression of an image is critical. A good impression of a map is helpful for stimulating related experience and background knowledge in the audience's mind, which is useful for understanding the information.

To improve the audience's impression of a map, we can improve the map similarity of map-like works, which is also an important issue in this field [35]. People have established a strong impression of map visualisation by long-term map use. The whole outline, region shape, and boundary structure in a map sheet have special cognitive patterns and impact map recognition. A familiar outline, similar to a true map, can help enhance the audience's psychological identification of the map [34]. Next, when people carry out in-depth observation, the internal regions of a map can be designed to facilitate the expression and transmission of information.

Map-like visualisation does not need to take into account physical and geographical features, which allows for great flexibility in its design. For instance, the shapes in a map-like visualisation can be adjusted as needed. We can make full use of the flexibility and freedom of the design process to select one appropriate form of representation. This study focuses on map shape design by considering two categories: the overall outline shape and the shape of internal regions.

A. OVERALL OUTLINE DESIGN

The overall outline is a significant attribute that people perceive from the whole. Compared with other properties,

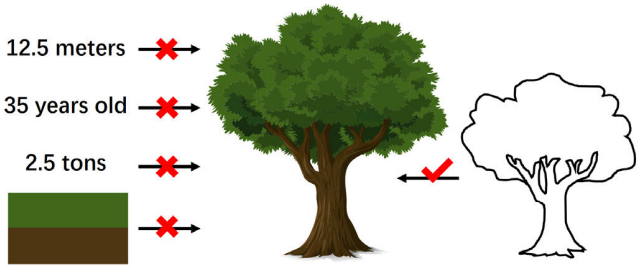

FIGURE 1. Inference of objects through attributes.

the outline can allow the audience to make more inferences about objects [33]. For example, in Figure 1, it is difficult to infer that the object is a tree if only one attribute value, such as height, age, weight, or colour, is given. However, when we give the approximate shape, even if the description is not very accurate and the size is not exactly the same, we can quickly associate it with a tree. In addition, the similar outlines between objects can help us in constructing the conceptual relationships between them. When the source object is used to understand the target object, this usage will undoubtedly promote our understanding of the concept and accelerate the processing of information [39], [47].

In the construction of the metaphorical relationships between two objects, it is important to construct a similar shape [48]. In the cognitive process, perceptual symbols such as shape are stored in the brain as cognitive experiences [1]. Given proper stimuli, they will be activated, even though these stimuli sometimes belong to cues rather than to precise descriptions [55]. For the audience, if the outline of an image is similar to that of a real map, then this similarity is beneficial for establishing the connection between them in the mind to strengthen the psychological identification of the map [2], [34]. This is critical for a map-like visualisation that aims to establish cognitive mapping between the map vehicle and the target ontology with the help of psychological association.

In the process of map-like visualisation design, we want to design the outlines of map-like works to make them similar to real map outlines. An approximate overall similarity is preferred over a precise fit because our purpose is to stimulate people's cognitive familiarity through a rough outline. There is no need to pursue high-precision similarity because the cost may be too large; thus, we can focus on the typical geometric features of the target object, for example, extracting the typical geometric features of the target object through map generalisation and adjusting the outline of the map-like work to make it move towards the simplified target object.

B. INTERNAL SHAPE DESIGN

Because a real map region always presents an irregular shape, a region that is too smooth or too regular (such as circles and squares) will weaken the relation between a map-like work and a real map in the audience's mind [34]. However, a region that has a shape that is too irregular will also cause a series of problems. Complicated and tortuous map regions not only

affect the beauty of a map but also result in cartographic and cognitive difficulty.

From the perspective of cartography, these complicated and tortuous internal regions are not conducive to the placement of map symbols, such as map annotations. The complicated and tortuous geometry compresses the space for map symbols, which limits the diversity of and dynamic changes in map symbols. This limitation has a very negative impact on subsequent cartography and dynamic map display. In addition, compared with a regular region that has the same area, the boundary of a complicated and tortuous region is longer, and the excessive occupancy of the space on the boundary will reduce the space utilisation rate.

In terms of cognition, map-like works often use the area to quantitatively express attribute values, reflecting the differences in abstract values through concrete geometric shapes. It is difficult to find the differences between attribute values by horizontally comparing the area when the map regions are too complicated and tortuous. The geometry of these regions often makes it difficult to concentrate on the targets, sometimes making them difficult to identify. In addition, complicated and tortuous regions may lead the audience to make unnecessary conjectures about their shape. All of these factors will affect the expression and cognition of information.

In summary, we hope that the shapes of the internal regions of maps are not too regular: they should be as simple as possible. Some related studies on TreeMap often prevent thin and elongated rectangles by controlling the aspect ratio [11]. In some map-like works, similar ideas can also be seen in region shape control [23], [53]. This study aims to balance the rule degree of the geometry in the map design of internal regions. To avoid map regions whose geometry is excessively regular, we explore relevant mapping technologies to ensure that the generated map regions have a certain randomness and variability. However, such randomness and variability may lead to the emergence of complicated and tortuous regions. Therefore, it is necessary to formulate certain rules with regard to shape constraints to avoid this issue.

III. APPROACH

We take the visualisation of hierarchical data as an example to explore the shape design of map-like visualisation. The structure of hierarchical data is very similar to that of maps. The hierarchical structure can be mapped to a choropleth map using polygon inclusion. To convert a hierarchical tree structure into a plane representation, we choose the Gosper curve to guide the regional subdivision and generate a map frame that is commonly used for the visual representation of hierarchical data [4], [46], [51].

The Gosper map takes regular hexagons as map construction units and realises a seamless splicing of the map regions. Diversified outline materials can be obtained by merging different map regions under the guidance of the Gosper curve. Because of the tortuous trend of the Gosper curve, the shapes of map regions are full of randomness, and there are many irregular regions. More importantly, Gosper maps have some potential for manipulation. A Gosper curve can be used as a control tool to adjust the relationship between the source data and the map data. At this point, the Gosper curve becomes the intermediate control layer.

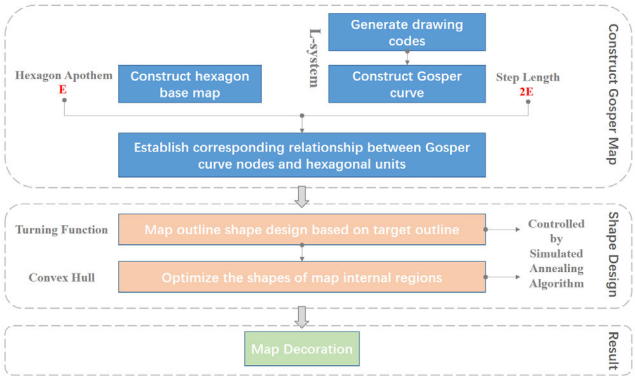

FIGURE 2. Flow chart of the method.

TABLE 1. Gosper drawing codes of different iterations.

Iteration	Drawing codes
1	A
2	A-B--B+A++AA+B-
3	A-B--B+A++AA+B-- +A-BB--B-A++A+B-- +A-BB--B- A++A+B+A-B-- B+A++AA+B-++A-B- -B+A++AA+B-A-B-- B+A++AA+B-++A- BB--B-A++A+B-
...	…

In this study, we aim to explore how to formalise the cartographic rules and constraints to meet the needs of docking with the intermediate control layer, and we input these rules and constraints into the intermediate control layer. In this way, cartographers can implement their design ideas in the mapping process. The flow chart of the methods in this study is shown in Figure 2, according to which we will introduce these methods in detail in the following.

A. CONSTRUCTING THE GOSPER MAP

In generating a Gosper map, first, the Gosper curve is constructed. In this study, the Gosper curve is generated by the L-system [29], which essentially replaces the initial character codes continuously to produce the drawing codes. Then, the Gosper curve can be constructed by geometrically interpreting the drawing codes.

The initial character code of the Gosper curve is "A". The replacement rule is to replace "A" in the string with "A-B–B+A++AA+B-" and to replace "B" with "+A-BB–B-A++A+B". This character code replacement is iteratively performed. As Table 1 shows, the drawing

TABLE 2. Geometric interpretation of the drawing codes.

Drawing codes	Geometric interpretation
A *B*	A straight line drawing with a length of one step
+	60-degree clockwise rotation of the drawing direction
-	60-degree counter-clockwise rotation of the drawing direction

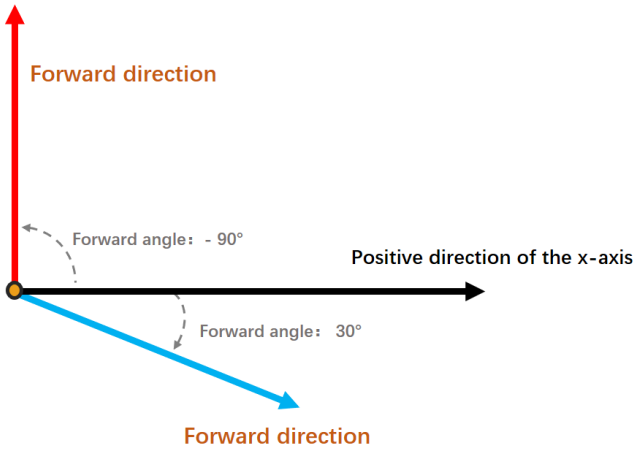

FIGURE 3. Forward angle illustration.

codes will become more complex as the number of iterations increases. Table II presents the geometric interpretation of drawing codes that can be used to draw the result curve.

It is necessary to determine the initial point and the initial forward angle first when constructing Gosper curves based on drawing codes. In particular, the forward angle is the angle from the positive direction of the x-axis to the forward direction of the curve (see Figure 3). The clockwise angle is positive, and the counter-clockwise angle is negative. In the process of curve drawing, when encountering "+", the forward angle is increased by 60 degrees; when encountering "-", it is reduced by 60 degrees. Given the coordinates (X_1, Y_1) of any known node on the Gosper curve, the coordinates (X_2, Y_2) of the next node in the forward direction can be calculated by Formula (1) and Formula (2). In these two formulas, L represents a length of one step of the curve, and θ represents the current forward angle. The coordinates of all nodes can be calculated in this way, and the result curve can be obtained by sequentially connecting these nodes.

$$X_2 = X_1 + L \times \cos(\theta) \tag{1}$$

$$Y_2 = Y_1 - L \times \sin(\theta) \tag{2}$$

As Figure 4 shows, Gosper curves constructed by drawing codes with different iterations grow iteratively. Figure 4 (a)

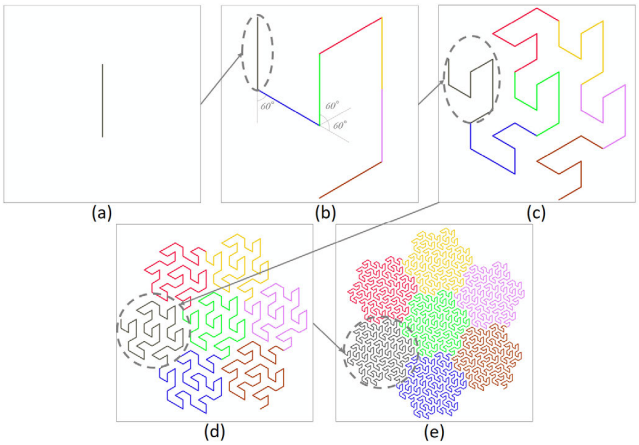

FIGURE 4. Iterative construction of the Gosper curve.

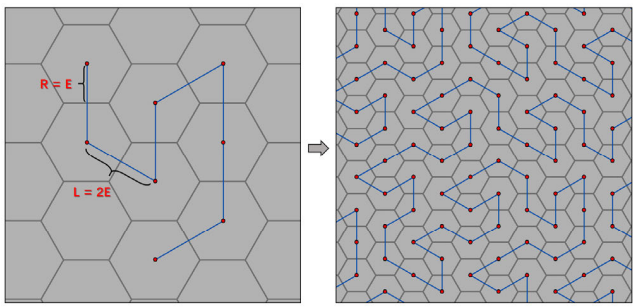

FIGURE 5. Establishment of the corresponding relationship between the Gosper curve and the hexagonal grid.

is the initial state of the Gosper curve, which corresponds to the initial code. The iterative growth of the Gosper curve in Figure 4 (b) can be realised by continuously rotating and splicing the minimum construction unit in Figure 4 (a). In this way, the result curve of each iteration can be used as the minimum construction unit of the next iteration; thus, the Gosper curve can be iteratively constructed.

The Gosper curve has a good coupling relationship with the regular hexagon grid [52]. As Figure 5 shows, for a hexagonal grid composed of hexagons whose apothem R is E, the step length L of the Gosper curve is set to $2E$, and the centre point of one hexagon is chosen as the starting point. In this way, the nodes of the Gosper curve can correspond to the centre points of the hexagons one by one, which can establish the corresponding relationship between the Gosper curve and the hexagonal grid. Therefore, the Gosper curve can be used to guide the division of a hexagon base map.

Based on the guidance order of the Gosper curve, a certain number of hexagons are selected to form map regions. Then, some attribute values can be expressed by the map area. For instance, based on the total attribute value, attribute value U, represented by each hexagonal unit, can be calculated. As shown in Formula (3), J represents the sum of the attribute values, and N indicates the total number of regular hexagons that compose this map. For each node of the hierarchical data, the number of hexagons needed can be calculated

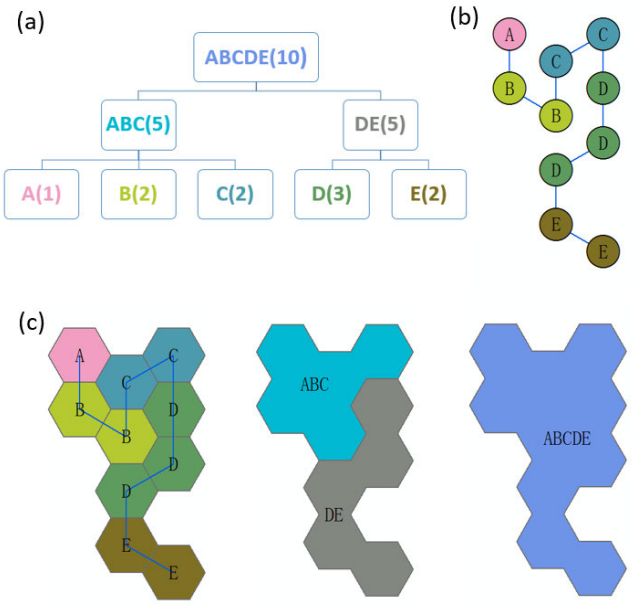

FIGURE 6. Construction of a Gosper map based on hierarchical data. [(a) Obtain the original hierarchical data; (b) arrange the leaf nodes of the hierarchical data on the Gosper curve; and (c) build the map regions from the bottom up.]

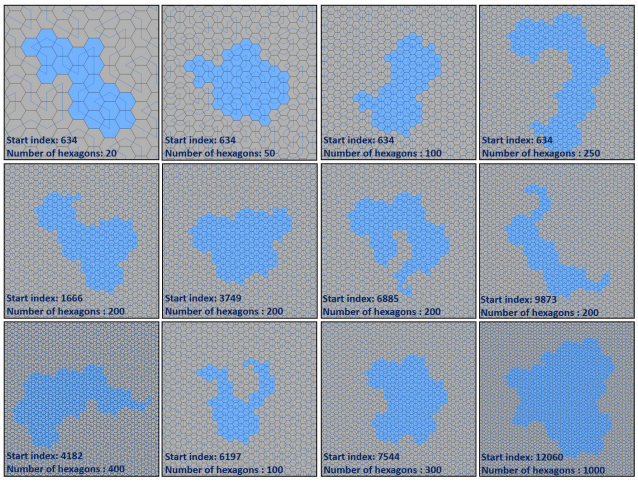

FIGURE 7. Different outline shapes, as determined by the start node index in the Gosper curve and the number of hexagons. (First row: keep the start node unchanged; second row: keep the number of hexagons unchanged; third row: Both the start node and the number of hexagons change.)

by the attribute value of the node. By merging these hexagons, the corresponding region of the node can be obtained.

The division of regions and the establishment of the hierarchical structure of the map are shown in Figure 6. Figure 6 (a) represents hierarchical data and the number of hexagons needed in each node. The leaf nodes of the hierarchical data are sequentially extracted. For each leaf node, the corresponding number of hexagonal units is assigned under the guidance of the Gosper curve, which is shown in Figure 6 (b). As Figure 6 (c) shows, according to the node inclusion relation, the parent node region can be obtained by fusing the sub-node regions. This process can be repeated from the bottom up to complete the division of each node region and to obtain the nested structure in the map.

$$U = \frac{J}{N} \tag{3}$$

B. MAP OUTLINE SHAPE DESIGN

Usually, map-like visualisations can obtain final outlines only after the maps are generated. In this study, a Gosper map can delineate the outline first, and then, we proceed to the subsequent mapping process. This unique advantage makes it possible to design and control the shape of the outline. In the process of mapping, the outline of a Gosper map is determined by two factors: the start node index in the Gosper curve and the number of hexagons. Since the nodes of the Gosper curve correspond to the hexagons of the base map one by one, we first choose the starting node index on the Gosper curve and then choose the corresponding number of hexagons based on the curve guidance order to form the set. The outline of the map can be obtained by extracting the outer boundary of the region corresponding to the hexagon set.

In the above process, when the start point is determined, different numbers of hexagons will generate different region shapes (see the first row in Figure 7). As the second row in Figure 7 shows, a different start node index corresponds to map outlines with different shapes if the number of hexagons is determined. When both the start node index and the number of hexagons change, the shapes of the regions change more (see the third row in Figure 7). In summary, changes in the start node index and the number of hexagons result in a disturbance of the outline shape. We define the map outline as $O(S, N)$, where S indicates the start node index and N is the number of hexagons. Using different settings of these two parameters, map outlines with different shapes can be generated. A large number of map outlines also provides rich material for outline design.

Our goal is to screen out an outline that is similar to the target shape from a large number of candidate outlines; thus, we need to choose a shape as the target. Then, the similarity between the candidate outline and target shape is continuously investigated by shape measurement. However, the location, slope angle, and area size of a candidate outline may not be consistent with the target outline due to the large amount of randomness in the Gosper map. Therefore, the shape measurement algorithm must satisfy the condition that it will not change with the translation, rotation and scaling of the shape. The turning function algorithm (Arkin et al., 1990) can effectively meet these requirements, and this study uses it to conduct a similarity measurement.

The turning function expresses the polygon by measuring the angle along a certain reference direction as a function of the arc length. Its basic principle is as follows: select a starting point on a polygon and a moving point that slides

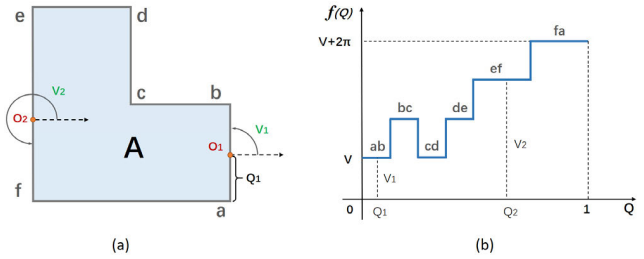

FIGURE 8. One-dimensional expression of a polygon based on the turning function.

counter-clockwise along the polygon boundary; the arc length of the moving point from the starting point is Q, the counter-clockwise tangent angle of the moving point along the reference direction (e.g., positive direction of x-axis) is V, and the turning function $f(Q) = V$ indicates the relationship between tangent angle V and arc length Q when the moving point moves along the boundary of the polygon. At the turns of the polygon boundary, the value of $f(Q)$ will change, increasing at the left-hand turns and decreasing at the right-hand turns. For instance, for polygon A in Figure 8 (a), point a is set as the starting point; moving point O_n moves counter-clockwise along the polygon boundary, the arc length from point a of moving point O_1 on edge ab is Q_1, the tangent angle along the reference direction (positive direction of x-axis) is V_1, and thus, the turning function value is $f(Q_1) = V_1$. The arc length of moving point O_2 on edge ef is Q_2, and the tangent angle along the x-axis is V_2; thus, we obtain $f(Q_2) = V_2$. By normalising the arc length, the turning function becomes a piecewise function in [0,1]. In this way, a two-dimensional polygon can be transformed into one-dimensional expression, as shown in Figure 8 (b).

For polygons A and B, their turning functions are $f_A(Q)$ and $f_B(Q)$, respectively, and their shape similarity can be measured by Formula (4). However, Formula (4) is very sensitive to the rotation of the polygon and the choice of the starting point on the boundary. In general, the minimum turning function value affected by all these changes in rotation and the starting point is used as the similarity measure between polygons A and B. Formula (5) describes the similarity of two polygons in two-dimensional space. In Formula (5), $f_A(Q+t)$ indicates the movement of the starting point along the boundary of polygon A by length t, while $f_A(Q) + \theta$ indicates the rotation of the polygon by angle θ. The smaller the value of $F(A, B)$ is, the greater the similarity between polygons A and B.

$$L_P(A, B) = \|f_A(Q) - f_B(Q)\|_P = \left(\int_0^1 |f_A(Q) - f_B(Q)|^P ds\right)^{\frac{1}{P}} \tag{4}$$

$$F(A, B) = \sqrt{\min_{\theta \in \Re, t \in [-1,1]} \int_0^1 [f_A(Q + t) + \theta - f_B(Q)]^2 ds} \tag{5}$$

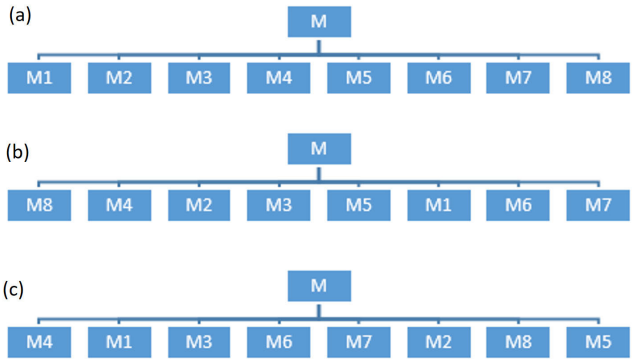

FIGURE 9. Hierarchical trees of different node orders.

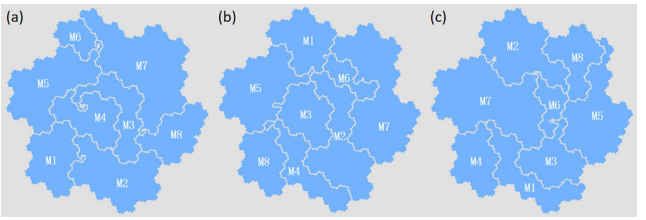

FIGURE 10. Different region shapes caused by different node orders.

C. INTERNAL MAP SHAPE DESIGN

Guided by the Gosper curve, the Gosper map completes the division of its internal regions, showing different region shapes. According to the principle of Gosper map making, the shapes of its internal regions depend on two factors: the area of the region, that is, the number of hexagons it contains, and the position of the two-dimensional plane of the internal region. In general, the area of the region is fixed; thus, its shape is determined by the position of the two-dimensional plane of the region. The nodes in the hierarchical tree are sequentially mapped to the Gosper curve, and their regions are divided under the guidance of the Gosper curve. Therefore, the position of the two-dimensional plane of each region is related to the position of its corresponding node in the hierarchical tree. This means that the shapes of map regions can be adjusted by changing the relative positions of the nodes in the hierarchical tree. For example, the original node order of the hierarchical tree is shown in Figure 9 (a), and its corresponding Gosper map is shown in Figure 10 (a). By adjusting the order of the nodes, we obtain the two hierarchical trees in Figure 9 (b) and Figure 9 (c); correspondingly, the Gosper map will also become Figure 10 (b) and Figure 10 (c). The node regions have the same area size, but different order positions tend to show different shapes. Notably, changing one node location will affect the region shapes of its sibling nodes that belong to the same parent node, thus creating a new map.

As shown in Figure 11, there are map regions with the same number of hexagons. The shapes in group (a) are too complicated and tortuous. In comparison, the overall shapes in

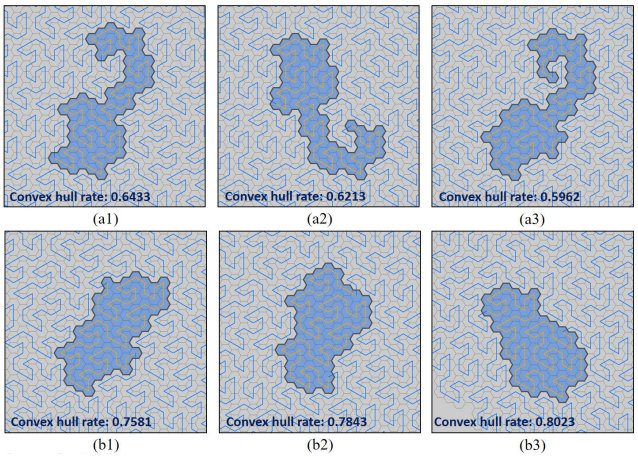

FIGURE 11. Two groups of regions with the same area.

group (b) are relatively simple. It is necessary to formulate a certain parameter to evaluate the shapes of the internal regions and to distinguish these two types of regions. Common aspect ratio constraints usually act to avoid excessive extension in a single direction. The complicated and tortuous region shape in this study is essentially due to the tortuous trend of the Gosper curve. The extension direction of these regions is not single but curly; thus, the aspect ratio parameter is not applicable. In addition, for the map regions in this study, the many depressions on their boundaries often result in their complicated and tortuous shapes. However, the convex hulls of these regions are usually relatively simple in shape. Therefore, the parameter of the convex hull rate (Formula (6)) is designed to evaluate the geometric complexity of map internal region M_i ($i \in \{1,2\ldots n\}$).

In Formula (6), P is the area measurement function, and C_{Mi} represents the convex hull of region M_i. Clearly, when the boundary shape of the region is too complex or the region contains many tortuous and narrow parts, the convex hull ratio will become very small. The closer the value of $V(M_i)$ is to 1.0, the simpler the region shape will be. In Figure 11, two groups of regions with the same area are calculated using the convex hull rate. Figure 11 shows that the values of the regions in group (a) are small, while those in group (b) are large, which indicates that the regions in group (b) are more in line with the needs of this study regarding region shape and are also consistent with the results of visual judgement. Because a change in one node location will also affect the region shapes of other sibling nodes of the same parent node, it is necessary to evaluate the shapes of all regions. For polygon groups, we prefer the minimum value of the convex hull rate of all regions (see Formula (7)) as the overall evaluation index of the region shape. The more closely F_v approaches 1, the more the overall region shape meets our needs.

$$V(M_i) = \frac{P(M_i)}{P(C_{M_i})}, \quad i \in \{1, 2...n\} \tag{6}$$

$$F_V = Min\{V(M_1), V(M_2), V(M_3)...V(M_n)\} \tag{7}$$

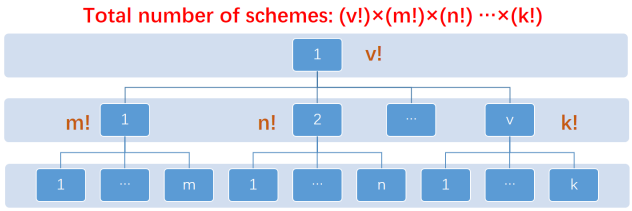

FIGURE 12. Calculation diagram of the number of design schemes.

The shapes of the regions in the map can be changed continuously by adjusting the locations of nodes in hierarchical data, and the regions that meet our needs can be selected to make the map regions as simple as possible. If there is only one layer of hierarchical data, then the map has $n!$ candidate internal region design schemes through the arrangement and combination of nodes, among which n is the number of nodes. When the number of layers of hierarchical data increases, the number of candidate schemes will increase greatly. Each parent node with n leaf nodes has $n!$ internal region design schemes. If these parent nodes are rearranged and combined, then the number of design schemes will increase again. As shown in Figure 12, the total number of map region design schemes for hierarchical data can be calculated by multiplying the factorial of the number of sub-nodes contained in each hierarchical node. When there are many layers or nodes in the hierarchical tree, the number of schemes will be very large.

D. COMPUTATION BY SIMULATED ANNEALING OPTIMISATION

The above discussion introduces the design essentials of the map outline and internal regions. There are a large number of solutions in the shape design process, including outline shape design and internal region shape design, due to the great degree of freedom in map-like visualisation. Selecting a scheme from the many candidate map results that satisfies our needs is a problem. If the selection process is carried out according to conventional methods such as enumeration, then the efficiency will be very low, as there are too many schemes. In this paper, a simulated annealing algorithm is introduced in the selection process.

The simulated annealing algorithm is a classical optimisation algorithm [26]. In theory, if the annealing is slow enough, it can achieve the global optimum [22]. In practice, it is easy to program and simple to implement with a small workload. For simulated annealing algorithms, it is necessary to set up the objective function using a certain rule constraint and then optimise it. In this study, the rule constraint is the specific shape requirements previously discussed, and the objective function is a quantitative representation of these requirements, such as Formula (5) and Formula (7). The simulated annealing algorithm generates a new solution by disturbing the current solution and uses the Metropolis criterion to determine whether to accept the new solution. The whole process is controlled by temperature. In the cooling

process of simulated annealing, some bad solutions will also be accepted with a certain probability to prevent the results from falling into the local optimum. In this study, a linear annealing schedule is adopted, i.e., the temperature is lowered by a linear coefficient, and a specified number of cycles are performed at each specific temperature.

For an outline shape, the target outline is defined as K, and we take the similarity function $F(O, K)$ between the candidate outline $O(S, N)$ and K as the objective function. The candidate outline parameters S (the start node index) and N (the number of hexagons) are continuously changed to generate new candidate outlines. At the same time, $F(O, K)$ is used to continuously calculate their similarity; the ultimate goal is to obtain a small value of $F(O, K)$ so that the corresponding map outline is similar to the target outline. The simulated annealing algorithm is used to control the aforementioned processes to optimise $F(O, K)$. The annealing process framework is as follows.

Arbitrary map outline $O(S, N)$ is selected as the initial solution. At the same time, $O_C(S, N)$ is the current solution. The value of objective function $F(O, K)$ is computed as initial energy E_C. Set initial temperature T_S and termination temperature T_E, build cooling model $T_{K+1} = a * T_K$ ($0 < a < 1$), and then set iteration number L at each temperature value. The temperature decreases continuously through the cooling model, and the following operations are performed L times at each temperature.

(1) Change the N and S in $O_C(S, N)$ to obtain new solution $O_{New}(S, N)$. Calculate E_T by $F(O_{New}, K)$. ΔE can be obtained by subtracting E_T from E_C.
(2) If $\Delta E > 0$, then accept the solution, set $O_C(S, N) = O_{New}(S, N)$, and set $E_C = E_T$; otherwise, perform step (3).
(3) Accept the solution with a certain probability. If $e^{\frac{E_C - E_T}{T_K}}$ is greater than a random number in a particular interval, then accept the solution, set $O_C(S, N) = O_{New}(S, N)$, and set $E_C = E_T$; otherwise, perform step (1) again.

In the above operations, the optimal value of the objective function is recorded, and the original optimal value is replaced by the newly generated optimal value. In addition, when there is no new optimal value in one round of cooling, it is considered to be an invalid cooling process and is recorded. When the temperature is lower than a certain threshold or the number of times of invalid cooling is higher than a certain threshold, the cooling process is stopped to output the results.

For an internal shape design, the simulated annealing frame is similar. The difference is that the order of nodes belonging to the same parent node is taken as a candidate solution. Random node sequence $S(M_1, M_2, M_3 \ldots M_n)$ is selected as the initial solution, which is also the current solution $S_C(M_1, M_2, M_3 \ldots M_n)$. According to the current node sequence, target function F_V can be calculated by Formula (7) to obtain initial energy E_C. New solutions are generated by perturbing the current solution through node position transformation. First, several nodes with the lowest convex hull rate are selected to adjust their positions, and they are randomly exchanged with the remaining nodes using the newly generated node sequence as a new solution. The number of selected nodes above is related to the number of nodes with the same parent node and the current temperature. The number of selected nodes is calculated by Formula (8), in which T_S is the initial temperature, T_K is the current temperature, and N is the number of nodes with the same parent node. In the initial stage of cooling, the adjustment of the node sequence is very strong. As the temperature decreases, the result tends to be stable, and the number of adjustment nodes grows increasingly lower. After setting the cooling model and relevant operating parameters, the iterative operation at each temperature is as follows.

(1) Transform the node sequence of current solution $S_C(M_1, M_2, M_3 \ldots M_n)$ to obtain $S_{New}(M_1, M_2, M_3 \ldots M_n)$ and calculate E_T by target function F_V. ΔE can be obtained by subtracting E_T from E_C.
(2) If $\Delta E < 0$, then accept the solution, set $S_C(M_1, M_2, M_3 \ldots M_n) = S_{New}(M_1, M_2, M_3 \ldots M_n)$, and set $E_C = E_T$; otherwise, perform step (3).
(3) Accept the solution with a certain probability. If $e^{\frac{E_C - E_T}{T_K}}$ is greater than a random number in a particular interval, then accept the solution, set $S_C(M_1, M_2, M_3 \ldots M_n) = S_{New}(M_1, M_2, M_3 \ldots M_n)$ and set $E_C = E_T$; otherwise, perform step (1) again.

$$G = \begin{cases} \dfrac{T_K \times N}{T_S \times 2}, & \dfrac{T_K \times N}{T_S \times 2} \geq 1 \\ 1, & \dfrac{T_K \times N}{T_S \times 2} < 1 \end{cases} \tag{8}$$

The recording form of the optimal result and the termination condition of the cooling are similar to those of the above outline design. However, the above operations are applied to the sub-regions of the same parent node, which means that these operations need to be performed for each parent region in the map. For hierarchical data with more than 2 layers, changing the parent region shape will affect the shapes of its sub-regions. If the sub-regions are adjusted first, when the shape of their parent region is adjusted, then this adjustment will damage the shapes of the sub-regions. Taking Figure 13 as an example, this map region in Figure 13 (a) has five sub-regions. If the sub-region shapes are adjusted first, as shown in Figure 13 (b), then change the parent region to another shape (see Figure 13 (c)). The adjusted sub-region shapes will also be affected and change accordingly as in Figure 13 (d). Therefore, to improve the efficiency of shape adjustment, in this study, the top-down regional adjustment strategy is adopted. First, the shapes of the top node regions are adjusted by the above method. For each region that has been adjusted, repeat the above operations for its sub-regions. By analogy, the process of regional adjustment is completed until all the leaf node regions at the lowest level are adjusted.

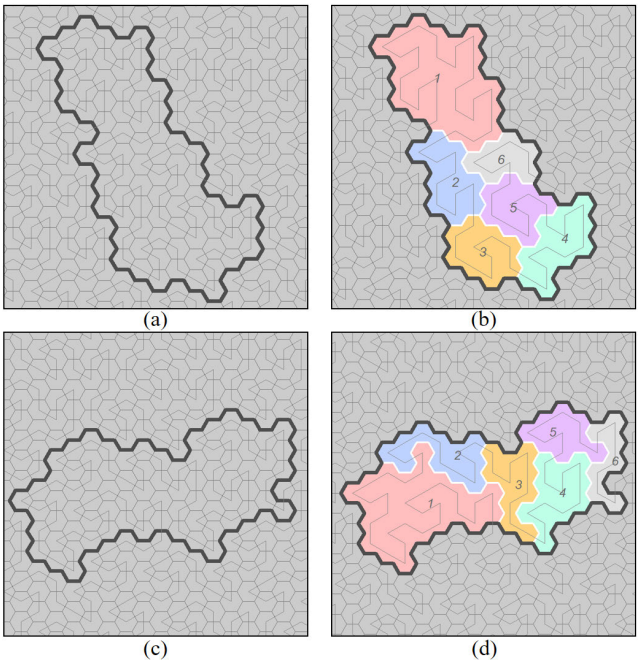

FIGURE 13. Bottom-up shape adjustment.

IV. EXPERIMENTS AND DISCUSSION

First, an outline shape design experiment is carried out. A set of regular hexagons can be obtained from the base map using the method introduced in Section III. The outline shape of these hexagons is similar to the shape of the target outline. Subsequently, combined with non-spatial hierarchical data, the internal regions are divided under the guidance of the Gosper curve, and the shapes of the internal regions are optimised. The above map outline design and internal region design are controlled by the simulated annealing algorithm.

A. EXPERIMENT IN MAP OUTLINE DESIGN

As shown in Figure 14 group (a), we chose the territories of France, China and Australia as our target outlines. To improve the efficiency of outline design, these data are all small-scale maps and do not contain many shape details. An intensive generalisation is carried out, and only the continental regions are preserved in the original data (see Figure 14 group (b)). The typical expression of the original shape is completed under the premise of maintaining the main structure of the outline.

The target outlines in Figure 14 were used to carry out three groups of experiments in which historical optimum values were continuously generated. We intercepted the slices in every experiment, as shown in Figure 15. These shapes are historically optimal outlines generated during the cooling process. As the value of the objective function decreases, the shape of the candidate outline is closer to the target outline (to facilitate the display, the candidate outline has been enlarged, shrunk, rotated, or turned). Finally, the ideal outline can be obtained.

FIGURE 14. Experimental data for map outline design. (Group a: Original data; group b: Data after generalisation).

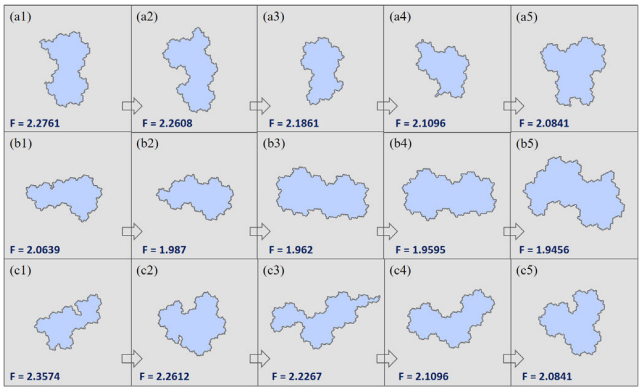

FIGURE 15. Experimental slices of outline shape optimisation.

There are many other space filling curves, and other common space filling curve types correspond to the regular quadrilateral grid, such as the Hilbert curve, the Peano curve, the Z-order curve, and quadratic Gosper curve. Similar to the Gosper map building rules, the above curve guidance can also be used to divide the corresponding regular quadrilateral base map into regions and to complete map construction. However, using a Z-order curve to construct a map will result in discontinuous regions because some adjacent nodes are too far apart from each other in space. As shown in the red box in Figure 16, when a part of the curve is filled, a jumping connection occurs. This occurrence will lead to an intermediate fracture of the generated map outline, which is not conducive to controlling the outline shape and will seriously affect the subsequent division of internal regions, as a result of which the same data item will correspond to two distant independent regions. Moreover, as the number of curve iterations increases, the distance between the above jumping connections will grow increasingly longer, as a result of which the two regions will grow increasingly farther apart. Therefore, we exclude the Z-order curve, construct maps using the Hilbert curve, Peano curve, and quadratic Gosper

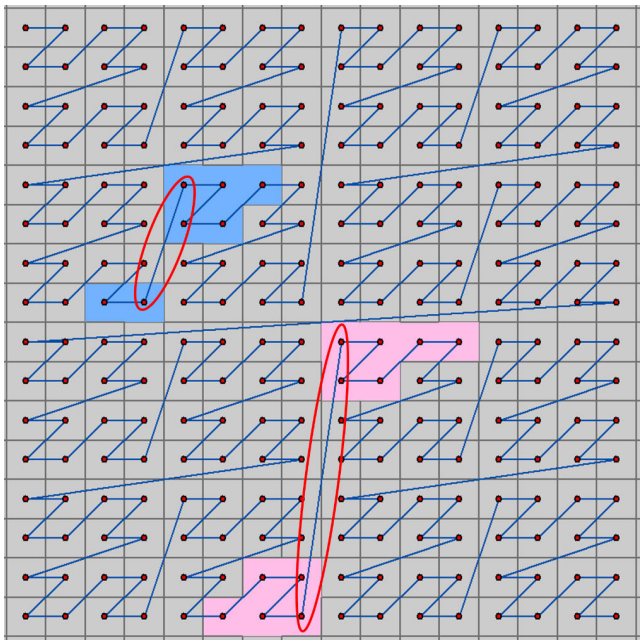

FIGURE 16. Discontinuous regions caused by jumping connections.

TABLE 3. Coding rules of the three space filling curves.

Curve name	Initial code	Replacement rule
Hilbert curve	A	A: -BF+AFA+FB- B: +AF-BFB-FA+
Peano curve	A	A: AFBFA-F-BFAFB+F+AFBFA B: BFAFB+F+AFBFA-F-BFAFB
Quadratic Gosper curve	A	A: AFA-BF-BF+FA+FA-BF-BFFA+BF+FAFABF-FA+BF+FAFA+BF-FABF-BF-FA+FA+BFBF- B: +FAFA-BF-BF+FA+FABF+FA-BFBF-FA-BF+FABFBF-FA-BFFA+FA+BF-BF-FA+FA+BFB

curve, design outlines using the same method as that used for the Gosper map, and perform comparative experiments.

The construction process of each curve is basically the same. That is, the curves also need to be generated by the L-system. The initial code and replacement rule of each curve are shown in Table 3. Notably, the code meanings of the Hilbert curve, Peano curve and quadratic Gosper curve are obviously different from those of the Gosper curve. In the codes, "A" and "B" have no specific meaning, and "F" represents a straight line drawing with a step length of one. In addition, "+" represents 90-degree clockwise rotation of the drawing direction, and "-" represents 90-degree counter-clockwise rotation of the drawing direction. When drawing curves, their coordinate calculation methods are the same as those of the Gosper curve. As Figure 17 shows, various kinds of curves with different levels of complexity can be

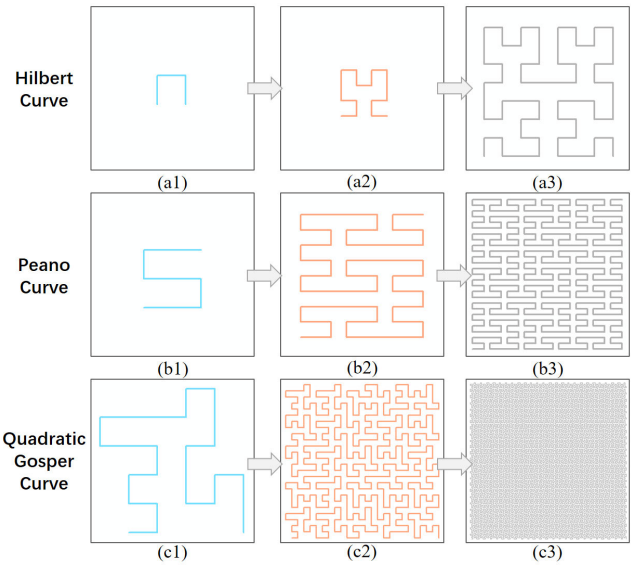

FIGURE 17. Three types of curves with different iterations.

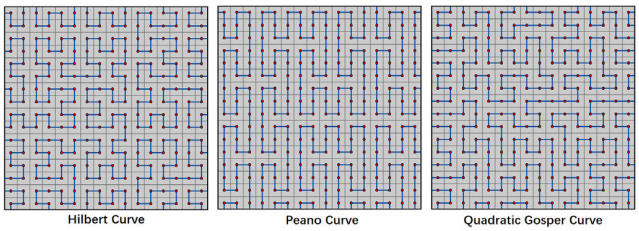

FIGURE 18. The correspondence between the curve nodes and regular quadrilateral grid units.

obtained through different iterations. In the construction of these curves, the step size of each curve is set to $2E$ for the grid composed of regular quadrilateral units with an apothem of E, and a centre point of one regular quadrilateral unit is chosen as the starting point. In this way, the one-to-one correspondence between the curve nodes and base map units can be established as shown in Figure 18, and outline shape optimisation can subsequently be carried out.

To promote the contrast, we use the same target outline to carry out the contrast experiments. Figure 14 (b3) is selected as the target outline for three types of map outline design. In the Hilbert map, Peano map and quadratic Gosper map, map outline design is controlled by the simulated annealing algorithm. Similar outline results are screened out by using a turning function to measure similarity. The map slices of the screening process are shown in Figures 19-21, in which the results of the outlines gradually approach the target outline.

However, in terms of visual effect, the outlines of the Hilbert map, Peano map, and quadratic Gosper map that constitute the final results are not as good as the outline that constitutes the final result in the Gosper map. For the target outline in Figure 14 (b3), the result in Figure 22 fits better than that in Figure 19 (e), Figure 20 (e) and Figure 21 (e). The map outlines designed by the three methods mentioned above have a serious defect, the universal right-angle phenomena.

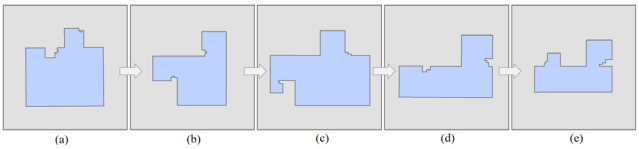

FIGURE 19. Map slices of the Hilbert map screening process.

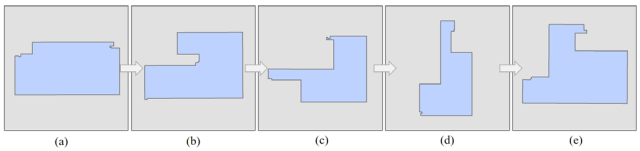

FIGURE 20. Map slices of the Peano map screening process.

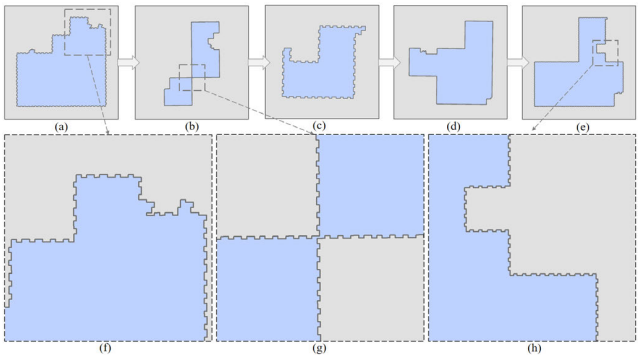

FIGURE 21. Map slices of the quadratic Gosper map screening process.

There are many straight lines and right angles in the outlines, which can result in a visually stiff region cut, making the map boundaries too regular and very different from the target outline in Figure 14 (b3). These phenomena are particularly serious in the outlines of the Hilbert map and Peano map (see Figures 19 and 20). Although the boundary of the outline in the quadratic Gosper map is not a pure straight line, Figures 21 (f)-(h), which are enlarged, show that the boundary is composed of very uniform jitter and, as a whole, is still linear.

The above phenomena are related not only to the trend of the guiding curve, which is too straight, but also to the shape of the regular quadrilateral unit used in the construction of the map regions. Under the combined effect of these two factors, the outline of the map is too regular at both the macroscopic and microscopic levels. In addition, as shown in Figure 21 (g), the outlines constructed in the quadratic Gosper maps sometimes have short and narrow neck regions, which are liable to cause visual discontinuity. Compared with the map outlines constructed under the guidance of the above curves, the Gosper map avoids scattered map outlines and ensures the integrity of the map. The tortuous trend of the Gosper curve prevents the map outline from being too regular. In addition, the use of hexagons as basic structural units in Gosper maps is further helpful with regard to these issues.

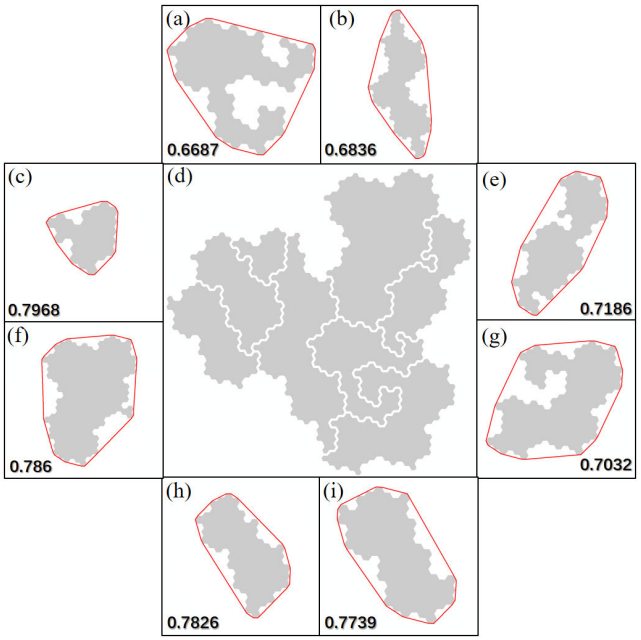

FIGURE 22. Map internal regions corresponding to the default node sequence.

B. EXPERIMENT IN INTERNAL MAP SHAPE OPTIMISATION

The experimental data are project application and support data from the National Natural Science Foundation of China in 2016. These typical hierarchical data have two levels: the department level and the discipline level. There are 8 departments in the first level, and each department contains several disciplines in the second level. The data attributes contain the number of approved projects, the approved funding amount, the funding rate and other information.

The Gosper curve and hexagon base map are cut by the outline of the result map to obtain the initial mapping data. Based on the approach introduced in Section III, guided by the Gosper curve, map regions are allocated according to an attribute such as the approved funding amount. First, regions for the bottom discipline nodes are allocated. Then, based on the inclusion relation, the location and shape of the region of each department are determined. The whole frame of the map is constructed in a bottom-up manner.

For the first-level internal regions of the map, as Figure 22 shows, a map made by the default node sequence has many tortuous concave regions. The convex hull ratios of these regions are obviously lower than those of other regions calculated by Formula (6). The shapes of these first-level map regions are adjusted to the satisfactory state with the help of the simulated annealing algorithm. The shape adjustment process is quantitatively expressed in Table 4. The minimum convex hull rate of all the map regions increases with the iterations. The whole annealing process will accept a certain number of bad solutions to prevent the results from falling into the local optimum. Figure 23 shows the number of accepted bad

TABLE 4. Shape adjustment experiment of the first-level internal regions of the map.

Iteration number	F_V
1	0.6687
21	0.6845
29	0.6946
251	0.6962
312	0.6973
336	0.6975
474	0.7186
1168	0.7287
1454	0.7335
6620	0.7378

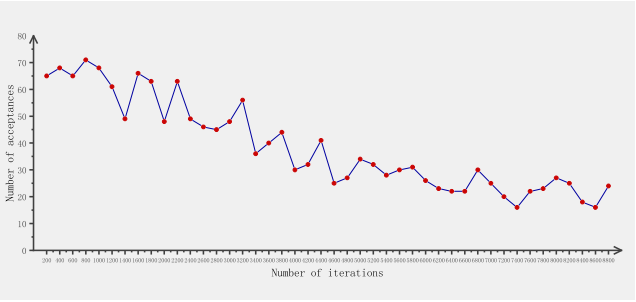

FIGURE 23. Line chart of accepted bad solutions (recorded every 200 iterations).

solutions during the cooling process, recording the number of accepted bad solutions every 200 iterations. Because the calculation of acceptance probability is influenced by random numbers, the line chart shows local oscillation. Overall, however, the number of accepted bad solutions is higher in the initial stage of cooling. As the cooling process proceeds, the results tend to be stable, and the number of accepted bad solutions decreases.

The map slices during the experiment are shown in Figure 24, in which regions of the same colour represent the same node objects. Changing the node order leads to a dynamic adjustment of the positions and shapes of the map regions. As F_V increases, the region shapes constantly adjust to the anticipated direction. Changing the location of a region affects not only the shape of the region but also the shapes of other regions. Because each region has been dynamically adjusting, the same region does not always have a good shape in the adjustment process; sometimes, its shape may not be as good as it was before. However, the overall effect of each new optimal solution will be improved, and the shapes of all the regions will finally achieve a satisfactory state.

After the shape optimisation of the first-level regions is completed, the second-level regions that they contain remain in their initial state. As shown in Figure 25, many sub-regions show obvious tortuous concave shapes. The second-level region shape optimisation is shown in Figures 26 and 27. For cases that have more sub-regions, as shown in Figure 26,

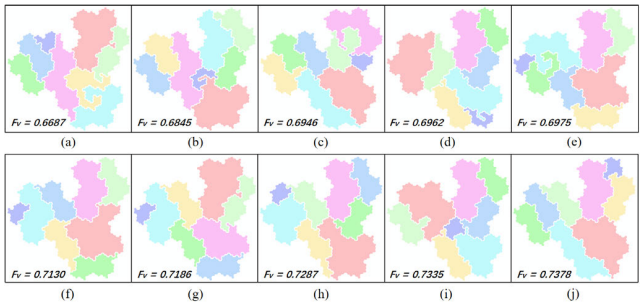

FIGURE 24. Map slices of the first-level region shape optimisation experiment.

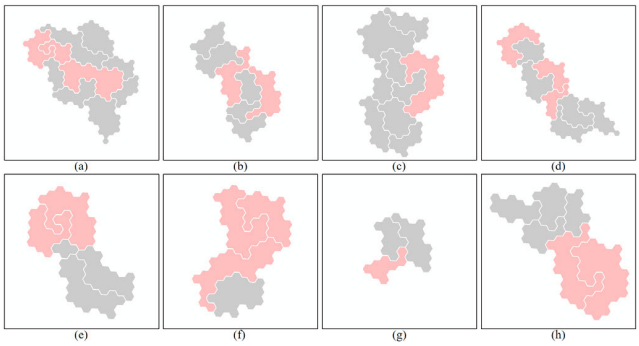

FIGURE 25. Second-level regions to be adjusted.

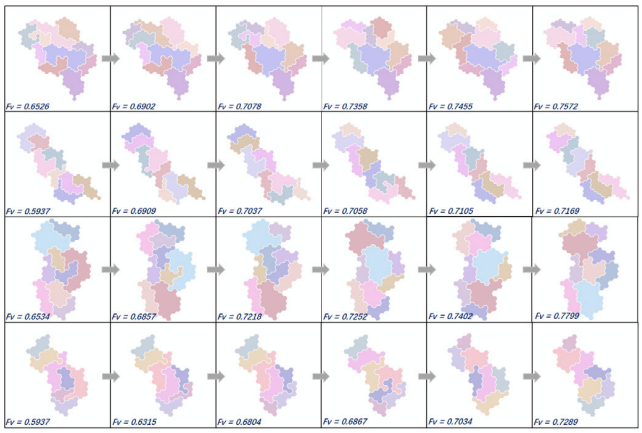

FIGURE 26. Map slices of the second-level region shape optimisation experiment (the cases that have more sub-regions).

changing the location of different regions will produce more map schemes, and there will be more optimal solutions accordingly. In addition, a larger number of regions and a larger area will make more changes in region shape, which will have a positive impact on the shape optimisation of this study.

Finally, all regions can be optimised in a top-down manner. On the one hand, because of the tortuosity of the Gosper curve, map regions that are excessively regular are avoided, and the map regions take on different shapes. On the other hand, controlled by the morphological parameter, the number of tortuous concave polygons is continuously reduced, and the shapes of all regions are optimised.

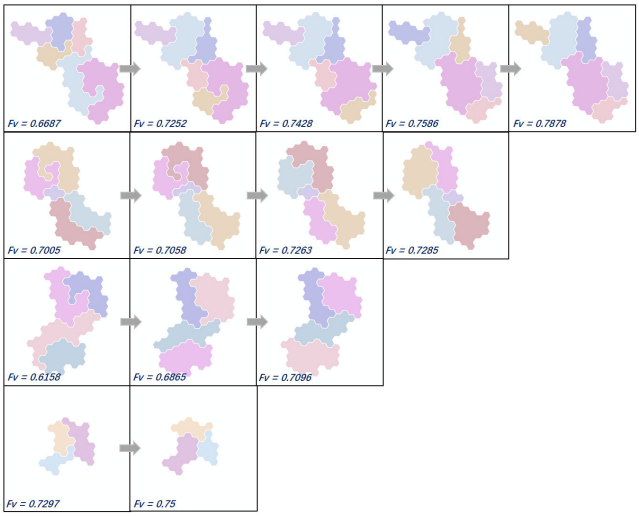

FIGURE 27. Map slices of the second-level region shape optimisation experiment (the cases that have fewer sub-regions).

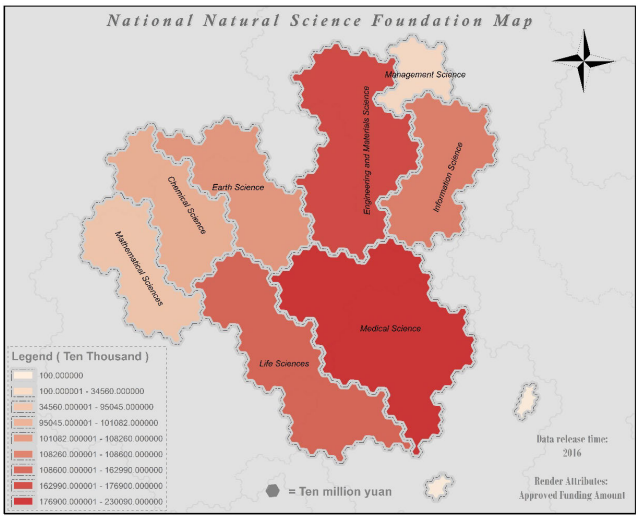

FIGURE 28. Result map after colouring.

C. MAP RENDERING

Through the above experiments, we complete the construction of the map framework. A geometric outline similar to a real map is obtained. To facilitate the transmission and comparison of attributes, the internal regions of the map are divided into simple geometric shapes. As a result, lateral contrast of the area is easily performed. In addition, the adjusted map regions are more suitable for label placement.

Next, the map is rendered and decorated. Abstract attribute values are expressed by colour and area. As shown in Figure 28, the approved funding amount of the department-level data is rendered by colour; the dark representation has a higher attribute value, and the light representation has a lower attribute value. To further enhance the object attribute contrast, map annotations, the legend and the symbol scale are added. The area and colour show that the medical science

FIGURE 29. Second-level map regions.

division, engineering and materials division and life sciences division have received the most financial support. In contrast, the management science division has an approved funding amount that is significantly lower than that of its sibling departments. To express the data hierarchy, different types of map boundaries are set and distinguished by style and colour. As Figure 29 shows, when the scale of the map is changed by enlargement, the map scene changes, showing more detailed information, and discipline-level data gradually emerge. At the discipline level, a similar horizontal comparison across disciplines can also be made. In the information science division, the colour of all sub-regions is generally darker, which means that these disciplines have all received high funding. In contrast, the subordinate disciplines in the management science division all receive less funding in general.

Map-like visualisation provides a new and vivid perspective for people to look at abstract non-spatial data. From the map, the audience can intuitively see the state's attention to human welfare and infrastructure-related fields, such as medicine and engineering. High input also appears in life sciences and information science fields that are related to technology. As it delivers information, this form of data presentation is also interesting to a certain extent, which helps attract a wider audience and thus facilitates the dissemination of information.

V. CONCLUSION

Map-like visualisation is a method of visualisation for representing abstract data using spatialization. On the one hand, the map-like design has a large degree of freedom to generate visualisation; on the other hand, it has to meet some requirements of the cartographic process. The shape design needs to consider a balance between these two facets. By using simulated annealing optimisation in the process of map construction, a map shape can be controlled according to the will of the map designer. Using a two-step shape control process for the exterior outline and internal regions, we can obtain a map outline that is close to a real form and simple internal regions of the map. This method can not only improve map similarity but also transfer metaphorical information through map features.

However, converting semantic information to simulated geo-entities is a difficult problem that requires a consideration of cartographic design requirements. This study takes into account only the shape issue in map design based on the Gosper curve. More map elements need to be studied to facilitate information transmission from the cognition perspective, such as symbol variable systems and map layer compositions. Not only does map-like design need to make the map-like function stand out through map visualisation, but it also has to prevent the map symbols from destroying the original semantic information. In addition, when the amount of data is very large, the shape design performance in this study will be affected. It is necessary to study methods to improve performance in this case to obtain satisfactory shape design results more quickly. In the future, we will further explore these aspects of map-like design to improve map-like visualisation.

REFERENCES

[1] T. Ai, X. Cheng, P. Liu, and M. Yang, "A shape analysis and template matching of building features by the Fourier transform method," *Comput., Environ. Urban Syst.*, vol. 41, pp. 219–233, Sep. 2013.

[2] T. Ai, S. Ke, M. Yang, and J. Li, "Envelope generation and simplification of polylines using delaunay triangulation," *Int. J. Geograph. Inf. Sci.*, vol. 31, no. 2, pp. 297–319, 2017.

[3] E. M. Arkin, L. P. Chew, D. P. Huttenlocher, K. Kedem, and J. S. Mitchell, "An efficiently computable metric for comparing polygonal shapes," in *Proc. 1st Annu. ACM-SIAM Symp. Discrete Algorithms*. Philadelphia, PA, USA: SIAM, 1990, pp. 129–137.

[4] D. Auber, C. Huet, A. Lambert, B. Renoust, A. Sallaberry, and A. Saulnier, "Gospermap: Using a gosper curve for laying out hierarchical data," *IEEE Trans. Vis. Comput. Graphics*, vol. 19, no. 11, pp. 1820–1832, Nov. 2013.

[5] J. Bertin, *Semiology of Graphics: Diagrams, Networks, Maps. Bertin, Jacques (Trans. W. J. Berg)*. Madison, WI, USA: Univ. Wisconsin Press, 1983.

[6] R. P. Biuk-Aghai and W. H. Ao, "A novel map-based visualization method based on liquid modelling," in *Proc. ACM 6th Int. Symp. Vis. Inf. Commun. Interact.*, 2013, pp. 97–104.

[7] R. P. Biuk-Aghai, P. C.-I. Pang, and Y.-W. Si, "Visualizing large-scale human collaboration in Wikipedia," *Future Gener. Comput. Syst.*, vol. 31, pp. 120–133, Feb. 2014.

[8] R. P. Biuk-Aghai, M. Yang, P. C.-I. Pang, W. H. Ao, S. Fong, and Y. W. Si, "A map-like visualisation method based on liquid modelling," *J. Vis. Lang. Comput.*, vol. 31, pp. 87–103, Dec. 2015.

[9] M. Blades, J. M. Blaut, Z. Darvizeh, S. Elguea, S. Sowden, D. Soni, C. Spencer, D. Stea, R. Surajpaul, and D. Uttal, "A cross-cultural study of young children's mapping abilities," *Trans. Inst. Brit. Geogr.*, vol. 23, no. 2, pp. 269–277, 1998.

[10] L. Boroditsky, "Metaphoric structuring: Understanding time through spatial metaphors," *Cognition*, vol. 75, no. 1, pp. 1–28, 2000.

[11] M. Bruls, K. Huizing, and J. J. van Wijk, "Squarified treemaps," in *Data Visualization*. Vienna, Austria: Springer, 2000, pp. 33–42.

[12] S. K. Card, A. Newell, and T. P. Moran, *The Psychology of Human-Computer Interaction*. 1983.

[13] S. Chen, S. Chen, Z. Wang, J. Liang, X. Yuan, N. Cao, and Y. Wu, "D-Map: Visual analysis of ego-centric information diffusion patterns in social media," in *Proc. IEEE Conf. Vis. Anal. Sci. Technol. (VAST)*, Oct. 2016, pp. 41–50.

[14] S. Chen, S. Chen, L. Lin, X. Yuan, J. Liang, and X. Zhang, "E-Map: A visual analytics approach for exploring significant event evolutions in social media," in *Proc. IEEE Conf. Vis. Anal. Sci. Technol. (VAST)*, Oct. 2017, pp. 36–47.

[15] S. Cheng and K. Mueller, "The data context map: Fusing data and attributes into a unified display," *IEEE Trans. Vis. Comput. Graphics*, vol. 22, no. 1, pp. 121–130, Jan. 2016.

[16] M. Dodge and R. Kitchin, *Mapping Cyberspace*, vol. 72. London, U.K.: Routledge, 2001.

[17] S. I. Fabrikant and B. P. Buttenfield, "Formalizing semantic spaces for information access," *Ann. Assoc. Amer. Geographers*, vol. 91, no. 2, pp. 263–280, 2001.

[18] S. I. Fabrikant, D. R. Montello, M. Ruocco, and R. S. Middleton, "The distance–similarity metaphor in network-display spatializations," *Cartogr. Geograph. Inf. Sci.*, vol. 31, no. 4, pp. 237–252, 2004.

[19] S. I. Fabrikant, D. R. Monteilo, and D. M. Mark, "The distance-similarity metaphor in region-display spatializations," *IEEE Comput. Graph. Appl.*, vol. 26, no. 4, pp. 34–44, Jul. 2006.

[20] S. I. Fabrikant and A. Skupin, "Cognitively plausible information visualization," in *Exploring Geovisualization*, vol. 3400. Amsterdam, The Netherlands: Elsevier, 2005, ch. 35, pp. 667–690.

[21] E. Gansner, Y. Hu, and S. Kobourov, "Visualizing graphs and clusters as maps," *IEEE Comput. Graph. Appl.*, vol. 30, no. 6, pp. 54–66, Nov./Dec. 2010.

[22] S. Geman and D. Geman, "Stochastic relaxation, Gibbs distributions, and the Bayesian restoration of images," in *Readings in Computer Vision*. San Mateo, CA, USA: Morgan Kaufmann, 1987, pp. 564–584.

[23] M. Gronemann and M. Jünger, "Drawing clustered graphs as topographic maps," in *Proc. Int. Symp. Graph Drawing*. Berlin, Germany: Springer, 2012, pp. 426–438.

[24] Z. Han, C. Cui, Y. Kong, F. Qin, and P. Fu, "Video data model and retrieval service framework using geographic information," *Trans. GIS*, vol. 20, no. 5, pp. 701–717, 2016.

[25] B. Jenny, J. Liem, B. Šavrič, and W. M. Putman, "Interactive video maps: *A year in the life of Earth's* CO_2," *J. Maps*, vol. 12, pp. 36–42, Mar. 2016.

[26] S. Kirkpatrick, C. D. Gelatt, and M. P. Vecchi, "Optimization by simulated annealing," *Science*, vol. 220, no. 4598, pp. 671–680, 1983.

[27] G. Lakoff and M. Johnson, *Metaphors we Live by*. Chicago, IL, USA: Univ. Chicago Press, 2008.

[28] S. Lee, S.-H. Kim, Y.-H. Hung, H. Lam, Y.-A. Kang, and J. S. Yi, "How do people make sense of unfamiliar visualizations?: A grounded model of novice's information visualization sensemaking," *IEEE Trans. Vis. Comput. Graphics*, vol. 22, no. 1, pp. 499–508, Jan. 2016.

[29] A. Lindenmayer, "Mathematical models for cellular interactions in development I. Filaments with one-sided inputs," *J. Theor. Biol.*, vol. 18, no. 3, pp. 280–299, 1968.

[30] C.-X. Ma, Y.-J. Liu, G. Zhao, and H.-A. Wang, "Visualizing and analyzing video content with interactive scalable maps," *IEEE Trans. Multimedia*, vol. 18, no. 11, pp. 2171–2183, Nov. 2016.

[31] C. J. Michael and B. Y. Lin, "Tile prediction schemes for wide area motion imagery maps in GIS," *ISPRS J. Photogramm. Remote Sens.*, vol. 133, pp. 30–36, Oct. 2017.

[32] D. R. Montello, S. I. Fabrikant, M. Ruocco, and R. S. Middleton, "Testing the first law of cognitive geography on point-display spatializations," in *Spatial Information Theory. Foundations of Geographic Information Science*. Berlin, Germany: Springer, 2003, pp. 316–331.

[33] M. J. Ortiz, "Visual rhetoric: Primary metaphors and symmetric object alignment," *Metaphor Symbol*, vol. 25, no. 3, pp. 162–180, 2010.

[34] P. C.-I. Pang, R. P. Biuk-Aghai, and M. Yang, "What makes you think this is a map?: Suggestions for creating map-like visualisations," in *Proc. VINCI*, 2016, pp. 75–82.

[35] P. C.-I. Pang, R. P. Biuk-Aghai, M. Yang, and B. Pang, "Creating realistic map-like visualisations: Results from user studies," *J. Vis. Lang. Comput.*, vol. 43, pp. 60–70, Dec. 2017.

[36] B. J. Phillips and E. F. McQuarrie, "Beyond visual metaphor: A new typology of visual rhetoric in advertising," *Marketing Theory*, vol. 4, nos. 1–2, pp. 113–136, 2004.

[37] J. Piaget, *Child's Conception of Space: Selected Works*, vol. 4. Evanston, IL, USA: Routledge, 2013.

[38] S. Sen, A. B. Swoap, Q. Li, B. Boatman, I. Dippenaar, R. Gold, M. Ngo, S. Pujol, and B. Hecht, "Cartograph: Unlocking thematic cartography through semantic enhancement," in *Proc. 22nd Int. Conf. Intell. User Interfaces (IUI)*, 2017, pp. 1–12.

[39] J. Schilperoord, A. Maes, and H. Ferdinandusse, "Perceptual and conceptual visual rhetoric: The case of symmetric object alignment," *Metaphor Symbol*, vol. 24, no. 3, pp. 155–173, 2009.

[40] A. Skupin, "From metaphor to method: Cartographic perspectives on information visualization," in *Proc. IEEE Symp. Inf. Vis. (InfoVis)*, Oct. 2000, pp. 91–97.

[41] A. Skupin, "A cartographic approach to visualizing conference abstracts," *IEEE Comput. Graph. Appl.*, vol. 22, no. 1, pp. 50–58, Jan. 2002.

[42] A. Skupin, "The world of geography: Visualizing a knowledge domain with cartographic means," *Proc. Nat. Acad. Sci. USA*, vol. 101, pp. 5274–5278, Apr. 2004.
[43] A. Skupin and B. P. Buttenfield, "Spatial metaphors for visualizing information spaces," in *Proc. ACSM/ASPRS Annu. Conv. Exhib.*, 1997, pp. 116–125.
[44] A. Skupin and S. I. Fabrikant, "Spatialization," in *The Handbook of Geographic Information Science*. 2007, pp. 61–79.
[45] A. Skupin, J. R. Biberstine, and K. Börner, "Visualizing the topical structure of the medical sciences: A self-organizing map approach," *PloS ONE*, vol. 8, no. 3, 2013, Art. no. e58779.
[46] F. Valsecchi, M. Abrate, C. Bacciu, M. Tesconi, and A. Marchetti, "DBpedia atlas: Mapping the uncharted lands of linked data," in *Proc. LDOW@ WWW*, 2015, pp. 1–6.
[47] L. van Weelden, R. Cozijn, A. Maes, and J. Schilperoord, "Perceptual similarity in visual metaphor processing," in *Proc. AAAI Spring Symp. Cogn. Shape Process.*, 2010.
[48] L. van Weelden, A. Maes, J. Schilperoord, and R. Cozijn, "The role of shape in comparing objects: How perceptual similarity may affect visual metaphor processing," *Metaphor Symbol*, vol. 26, no. 4, pp. 272–298, 2011.
[49] M. Wattenberg, "A note on space-filling visualizations and space-filling curves," in *Proc. IEEE Symp. Inf. Vis.*, Oct. 2005, pp. 181–186.
[50] J. Wood, P. Fisher, J. Dykes, D. J. Unwin, and K. Stynes, "The use of the landscape metaphor in understanding population data," *Environ. Planning B, Planning Des.*, vol. 26, no. 2, pp. 281–295, 1999.
[51] R. Xin, T. Ai, and B. Ai, "Metaphor representation and analysis of non-spatial data in map-like visualizations," *ISPRS Int. J. Geo-Inf.*, vol. 7, no. 6, p. 225, 2018.
[52] R. Xin, T. Ai, and B. Ai, "Encoding and compressing hexagonal raster data by the Gosper curve," *Trans. GIS*, to be published. doi: 10.1111/tgis.12569.
[53] M. Yang and R. P. Biuk-Aghai, "Enhanced hexagon-tiling algorithm for map-like information visualisation," in *Proc. ACM 8th Int. Symp. Vis. Inf. Commun. Interact.*, 2015, pp. 137–142.
[54] W. Yu, T. Ai, and S. Shao, "The analysis and delimitation of central business district using network kernel density estimation," *J. Transp. Geogr.*, vol. 45, pp. 32–47, May 2015.
[55] R. A. Zwaan, R. A. Stanfield, and R. H. Yaxley, "Language comprehenders mentally represent the shapes of objects," *Psychol. Sci.*, vol. 13, no. 2, pp. 168–171, 2002.

TINGHUA AI was born in Hubei, China, in 1969. He received the B.S., M.S., and Ph.D. degrees in cartography from the Wuhan University of Surveying and Mapping Science and Technology, Wuhan, in 1994 and 2000, respectively. He is currently a Professor with the School of Resource and Environmental Sciences, Wuhan University. His research interests include multi-scale representation of spatial data, map generalization, spatial cognition, and spatial big data analysis.

RUI XIN was born in Shandong, China, in 1991. He received the B.S. degree in geographical information systems from the Shandong University of Science and Technology, in 2014. He is currently pursuing the Ph.D. degree with Wuhan University. His research interests include map-like visualization, spatial data compression, and spatio-temporal data analysis.

XIONGFENG YAN received the B.Sc. and Ph.D. degrees in cartography and geoscience from Wuhan University, Wuhan, China, in 2015 and 2019, respectively. He is currently a Postdoctoral with the College of Surveying and Geo-Informatics, Tongji University, Shanghai, China. His main research interests include cartography and machine learning with special focus on the graph-structured spatial data.

MIN YANG was born in Hubei, China, in 1985. He received the B.S. and Ph.D. degrees in cartography from Wuhan University, Wuhan, in 2007 and 2013, respectively, where he is currently an Associate Professor with the School of Resource and Environmental Sciences. His research interests include change detection of spatial data, map generalization, and spatial big data analysis.

BO AI was born in Hubei, China, in 1979. He received the B.S. and M.S. degrees from Wuhan University, Wuhan, in 2005, and the Ph.D. degree in geographical information systems from the Shandong University of Science and Technology, Shandong, in 2011, where he is currently an Associate Professor with the College of Geomatics. His research interests include spatio-temporal modeling and visualization.